Real-Time Monitoring Distance Changes in Surfactant-Coated Au Nanoparticle Films upon Volatile Organic Compounds (VOCs).

*M. C. Dalfovo, L. J. Giovanetti, J. M. Ramallo-López, R. C. Salvarezza, F. G. Requejo, and F. J. Ibañez**

Instituto de Investigaciones Fisicoquímicas, Teóricas y Aplicadas (INIFTA). Universidad Nacional de La Plata - CONICET. Sucursal 4 Casilla de Correo 16 (1900) La Plata, Argentina.

Supporting Information

SAXS fitted curves of SNPs dispersed in toluene. SAXS curves were normalized to the intensity of the direct X-ray beam to compensate the constant decrease of X-ray emission of the synchrotron source. The SAXS intensity was determined as a function of the modulus of the scattering vector $q = (4\pi/\lambda)\,\mathrm{Sin}(\theta)$, with λ being the wavelength of the X-Ray beam ($\lambda = 0.161$ nm) and 2θ the scattering angle. A Pilatus detector recorded the SAXS curves. In order to reproduce the SAXS experimental curves, we have proposed a simple model consisting of a diluted solution of spherical objects.[1] A small dispersion of the NP radii - described by a LogNormal function - is allowed in the model and quantized by the distribution variance (σ) and the average diameter (D). This fit was performed using SASfit. As shown in figure S1, the experimental data could be well reproduced by assuming a dilute set of spherical particles, with no evidence of distance correlation between particles.

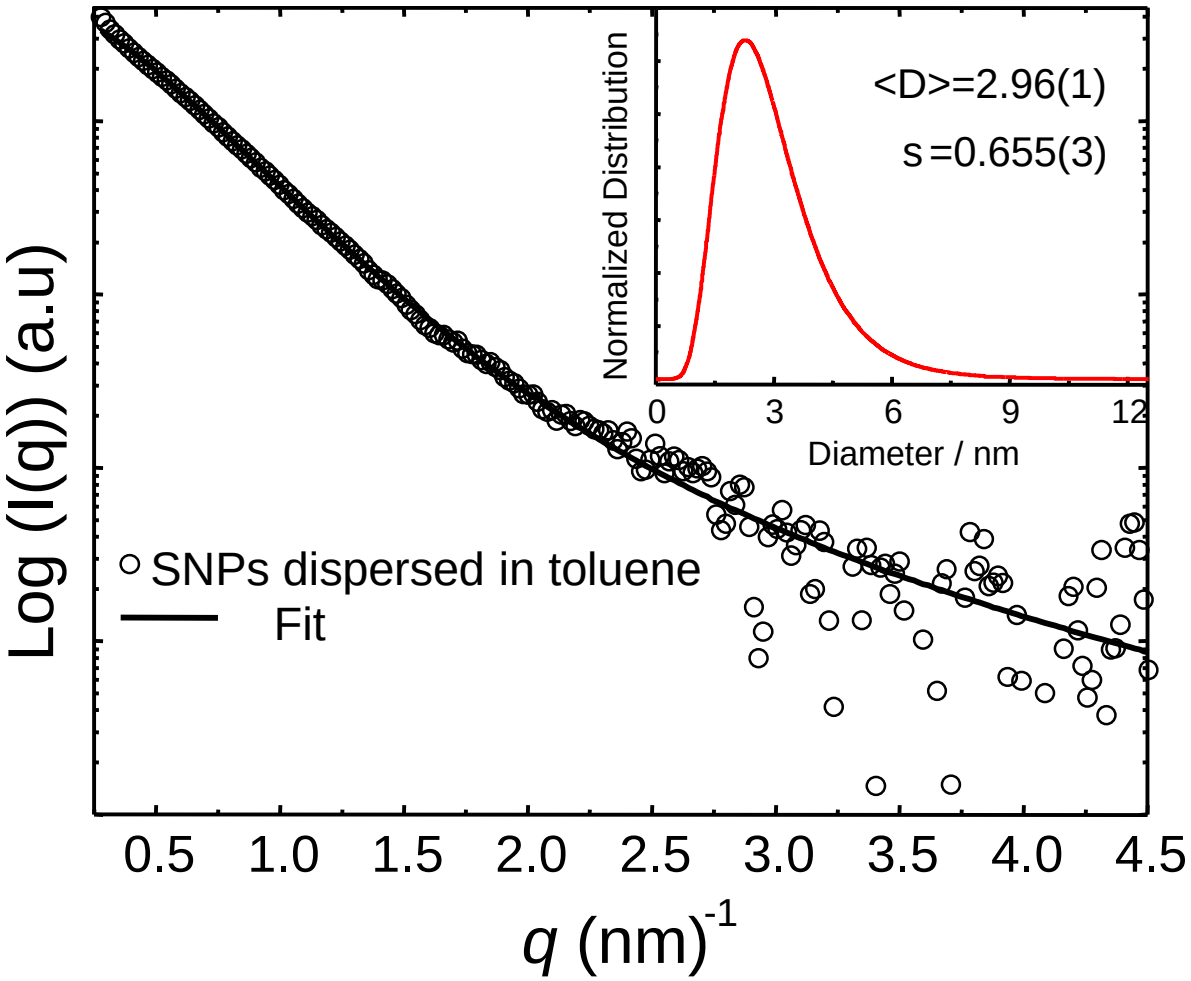

Figure S1. SAXS distribution (Inset) and no spatial correlation obtained from surfactant-coated Au nanoparticles (SNPs) suspended in toluene solution.

SAXS Plot of drop-cast deposited SNPs film on mica.

15 mm of mica disks (Attwater Co.) were used as substrates for SAXS characterization. Mica disks were cleaned and functionalized with APTES the same manner as GISAXS substrates. Later, 30 μL (1.1 mg/mL) of surfactant-coated Au NPs (SNPs) were drop-cast deposited on a clean mica disk. SAXS plot shows a long range of q values (from 0.7 to 1.1 nm^{-1}) indicating poor SNPs correlation.

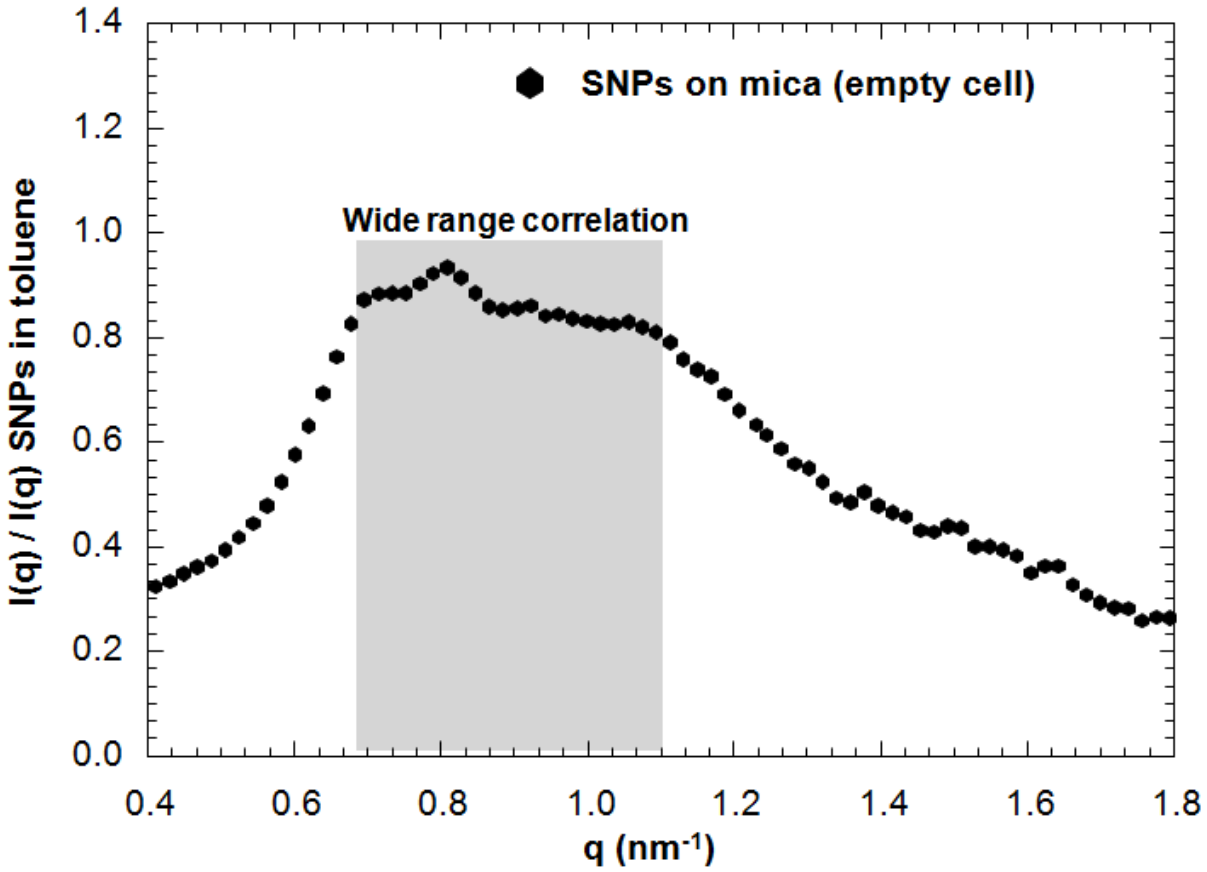

Figure S2. SAXS plot obtained from SNPs assembled by drop-casting onto a mica disk.

Experimental Set-up for GISAXS sensing

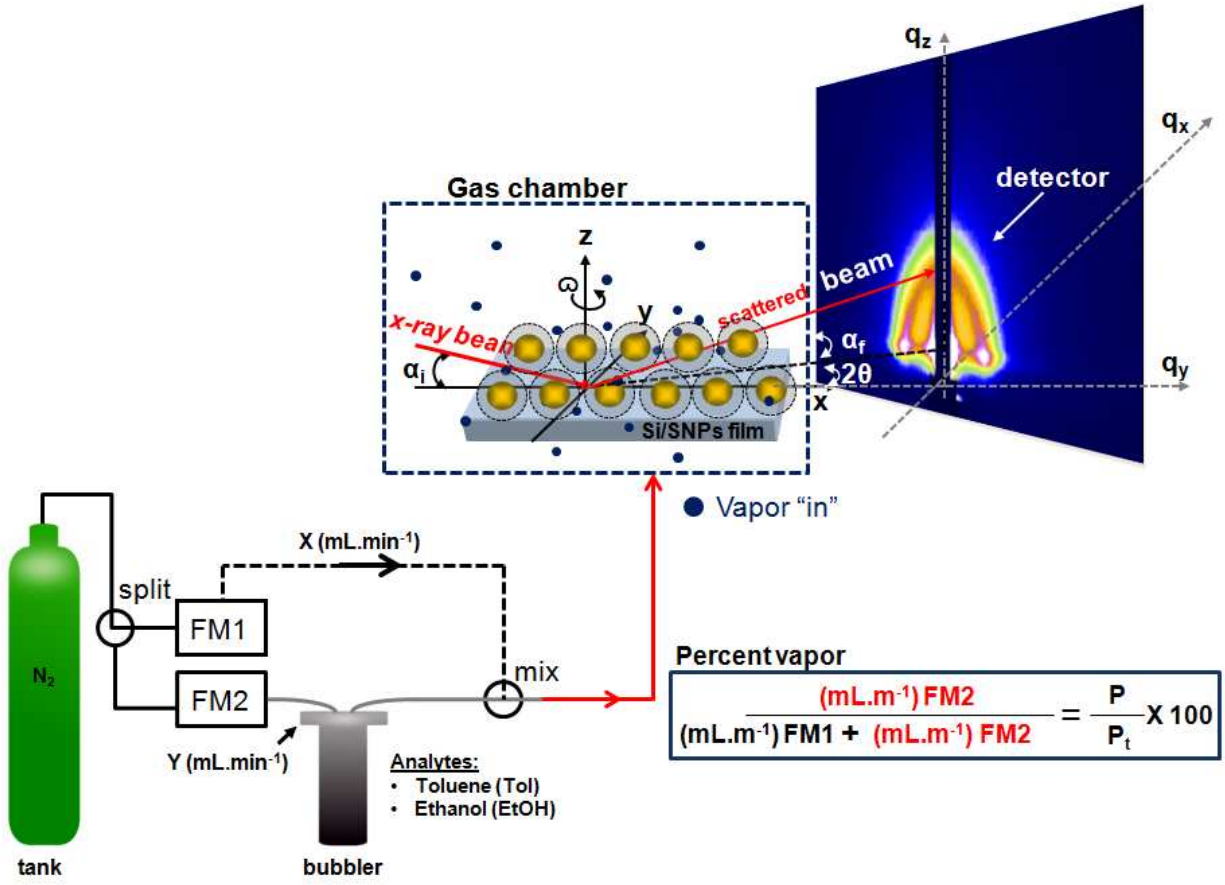

Figure S3. *In-situ* GISAXS experiment performed on a SNPs film exposed to different concentrations of ethanol (EtOH) and toluene (Tol) vapors previously mixed with N_2 gas. Vapor mixture concentration is controlled by the use of flow meters (FM) and its concentration in percent vapor calculated by the equation as indicated.

***In-situ* GISAXS evolution performed along the *y*-axis**

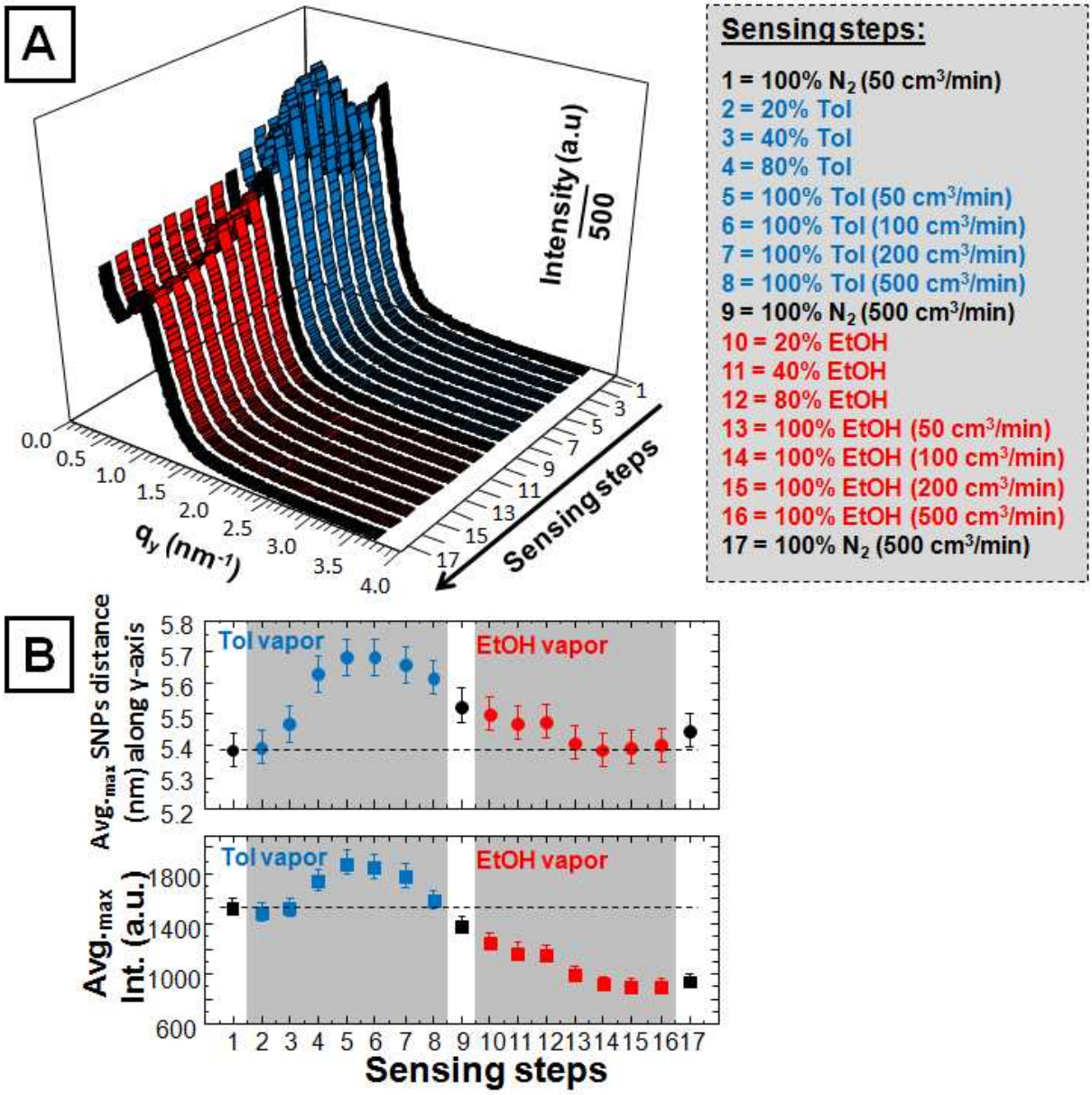

Figure S4. *In-situ* GISAXS plot (q_y versus intensity) performed on a selected as-formed SNPs film subjected to increasing concentrations and flows of Tol and EtOH as indicated in each step (a). The plot below shows *core-to-core* distance along y-axis (derived from q_y values) and average maximum ($Avg._{max}$) intensity upon each step as indicated (b).

GISAXS data along q_y and q_z axes.

Tol sensing along q_y

SNPs film	q_y max (nm^{-1})	Intensity (a.u.)	*core-to-core* distance (nm)[b]	Δ d (nm)[c]	Δ Intensity (a.u.)[d]	Δ Intensity %[e]	*edge-to-edge* distance (nm)[f]
Initial (step #1)	1.04	1547	5.4	/	/	/	2.4
Tol vapor (step #5)[a]	0.99	1888	5.7	0.3	341	22	2.7
Final (step #9)	1.01	1389	5.5	0.1	-158	-10	2.6

Tol Sensing along q_z

SNPs film	q_z max (nm^{-1})	Intensity (a.u.)	*core-to-core* distance (nm)[b]	Δ d (nm)[c]	Δ Intensity (a.u.)[d]	Δ Intensity %[e]	*edge-to-edge* distance (nm)[f]
Initial (step #1)	1.05	1215	5.3	/	/	/	2.4
Tol vapor (step #5)[a]	0.99	1744	5.6	0.3	529	44	2.7
Final (step #9)	1.03	1099	5.5	0.1	-116	-10	2.5

EtOH Sensing along q_y

SNPs film	q_y max (nm^{-1})	Intensity (a.u.)	*core-to-core* distance (nm)[b]	Δ d (nm)[c]	Δ Intensity (a.u.)[d]	Δ Intensity %[e]	*edge-to-edge* distance (nm)[f]
Initial (step #9)	1.03	1389	5.5	/	/	/	2.5
EtOH vapor (step #14)[a]	1.04	938	5.4	-0.1	-451	-32	2.4
Final (step #17)	1.03	954	5.4	0.0	-435	-31	2.5

EtOH Sensing Along q_z

SNPs film	q_z max (nm^{-1})	Intensity (a.u.)	*core-to-core* distance (nm)[b]	Δ d (nm)[c]	Δ Intensity (a.u.)[d]	Δ Intensity %[e]	*edge-to-edge* distance (nm)[f]
Initial (step #9)	1.03	1099	5.5	/	/	/	2.5
EtOH vapor (step #13)[a]	1.05	752	5.3	-0.1	-347	-32	2.4
Final (step #17)	1.03	796	5.4	0.0	-303	-28	2.5

Table S1. Data obtained by GISAXS of as-formed SNPs film during Tol and EtOH vapor sensing. Note that: (a) corresponds to the maximum change in *q* during vapor sensing, (b) *core-to-core* distance between nanoparticles using equation #1 presented in the main text, (c) distance difference between the indicated step with respect to initial step, (d) intensity difference between the indicated step and the initial step, (e) intensity percent change in this step with respect to the initial step, and (f) *edge-to-edge* distance was calculated according to the radius of a SNP (~1.5 nm) obtained from SAXS (see Figure S1).

SAXS measurements.

SAXS measurements were performed using the SAXS-1 beam line at Laboratório Nacional do Luz Síncrotron (LNLS), Campinas, Brazil. The SAXS intensity curves were determined using a 2D Pilatus detector as functions of the modulus of the scattering vector $q = 4\pi\sin\theta/\lambda$, ($\theta$) being half the scattering angle and (λ) the X-ray wavelength, $\lambda = 1.61$ Å. The SAXS curves were normalized to the intensity of the direct X-ray beam to compensate for the continuous decrease in emission of the synchrotron source. The solid-state films under study were placed inside a cell with two thin and parallel mica windows for transmission SAXS measurements and films exposed to air and pure solvents of EtOH and Tol. In the X-ray scattering process involving a system consisting of a set of identical nano-objects with spatial correlation, interference effects are relevant, so the simple equation for isolated nano-objects does not longer hold. These effects can be taken into account in a simple way for the particular case of a homogeneous set of spherical (or more generally centro-symmetrical) nano-objects. For this system, $I(q)$ is given by:

$$I(q) = N \cdot I_1(q) \cdot S(q)$$

Where $S(q)$ is the structure function. For a set of nano-objects without long-range order, $S(q)$ tends asymptotically to 1 at high q. Indeed, if the nano-objects are spatially uncorrelated and form a dilute solution, $S(q)$ is equal to 1 over the whole q domain, and the equation becomes similar to the one for isolated nano-objects.

Assuming that the $I(q)$ is the same as the one measured in solution, $S(q)$ could be obtained by[1]

$$S(q) = I_{correlated}(q) / I(q)$$

Figure S5 shows the obtained curves for *S(q)* in each case. The peak shadowed in gray indicates the q_{max} for the correlation region, assuming the same model as stated in the main text. It should be noted that SNPs film in air shows poor correlation, which sharpens as long as the film interacts with Tol and EtOH solvents. Consistent with GISAXS plots (main text), the intensity at q_{max} increases and decreases in the presence of Tol and EtOH indicating improvement and worsening of the SNPs correlation (order), respectively.

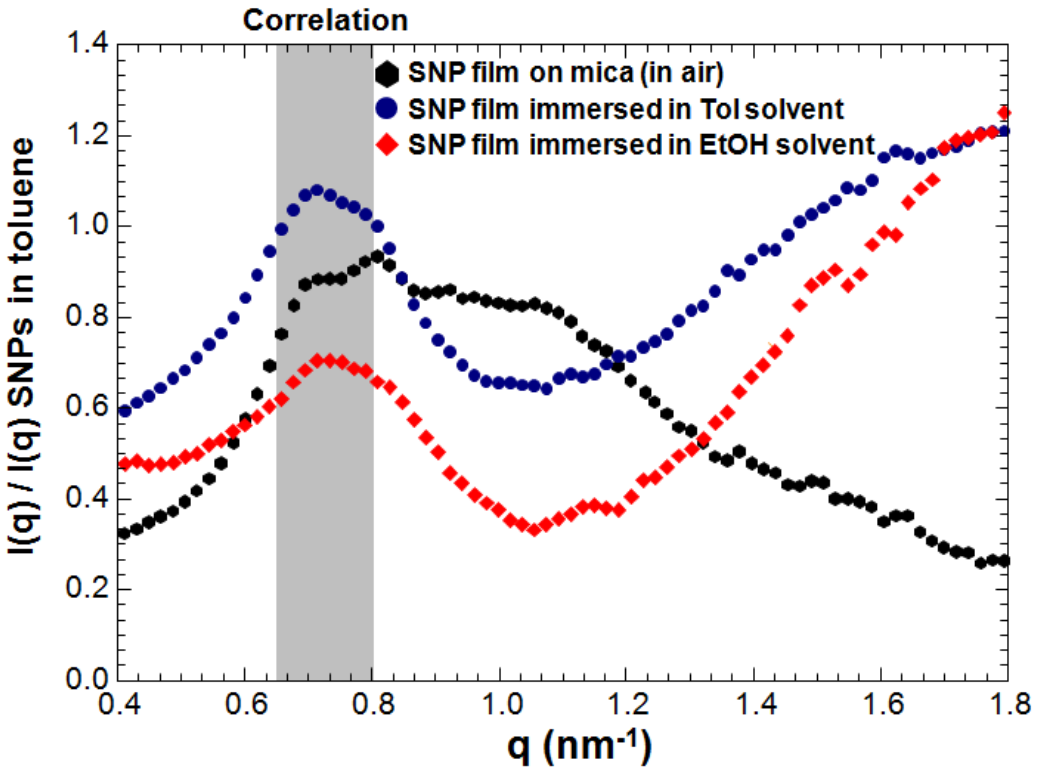

Figure S5. SAXS plot of SNPs film before (in air) and after exposure to Tol and EtOH solvents.

UV-vis of TOABr-coated Au NPs film treated with NDT and NT.

The Figure shows a selected SNPs film whose plasmon band red shifted after exchange with NDT and NT from 557 to 577 and 580 nm, respectively. A red shift is caused by an increase in refractive index (RI) and/or NPs distance shrinkage or agglomeration. Since NDT and NT may have similar RI, then changes in plasmon band should be solely attributed to plasmon coupling effects.[2] UV-vis results rule out cross-linking between Au cores because red shifting for NDT should have been more pronounced relative to that of monothiol (NT).[3] By the contrary, the plasmon shift for NDT- is slightly smaller than NT-treated film. The lesser degree of red shifting observed in NDT-treated film with respect to NT is consistent with GISAXS results, which exhibited NPs separation after incorporation of NDT into the film.

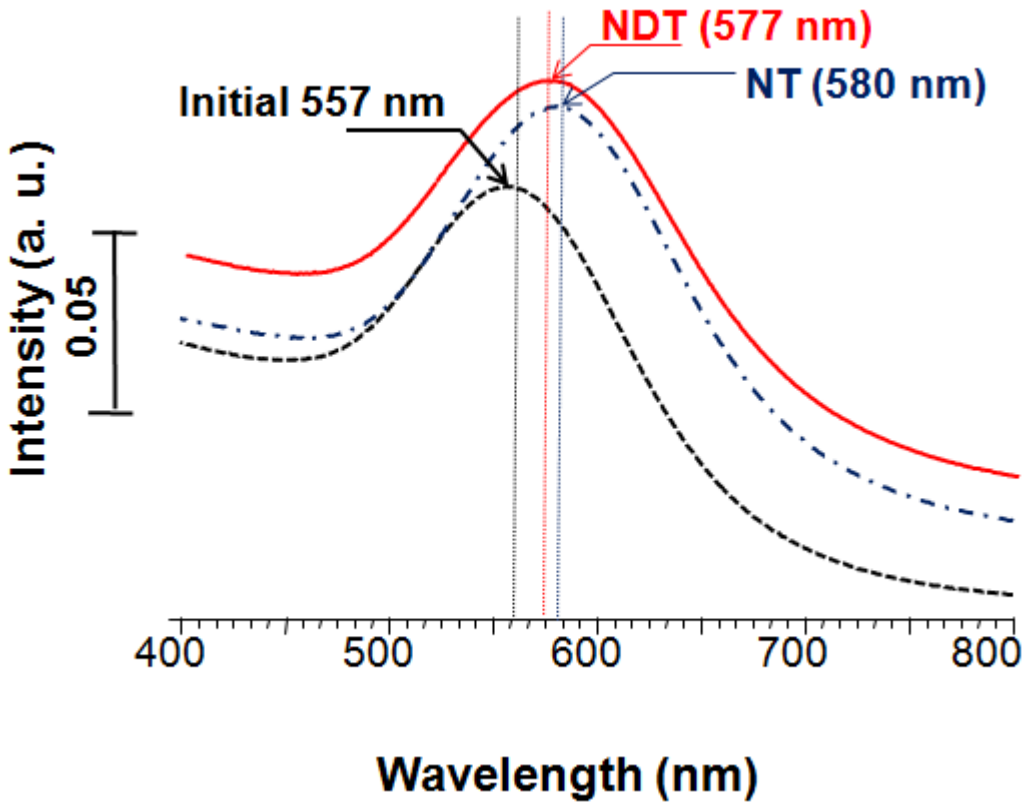

Figure S6. UV-vis plots indicating similar red shifts values ~577 and ~580 nm after exchange with NDT and NT, respectively. This suggests no cross-linking between adjacent cores consistent with inter-NPd obtained by GISAXS.

Scheme.

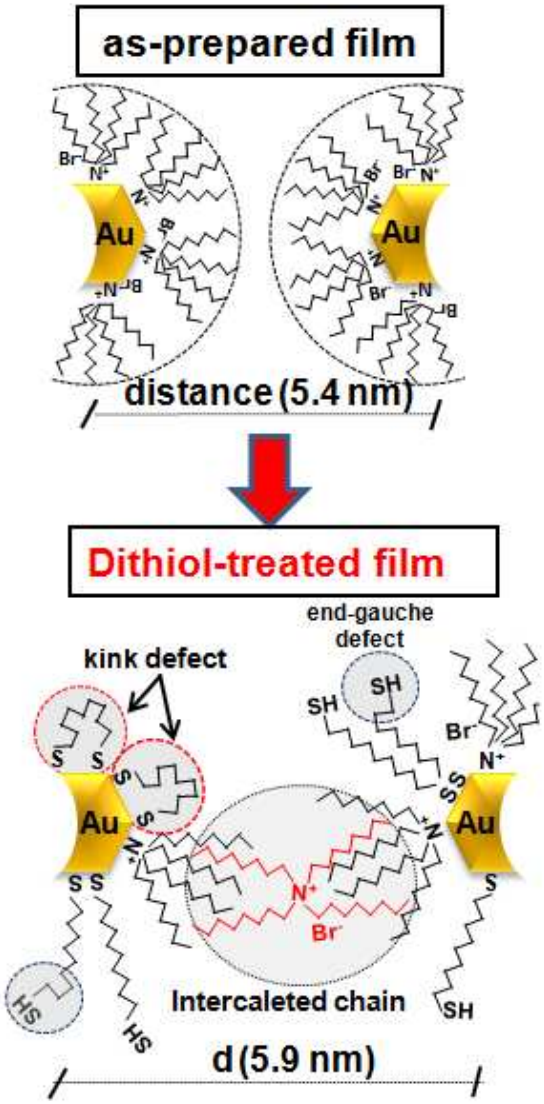

Scheme S7. Suggested scheme of a single TOA^+ ligand intercalated and interdigitated between two surfactant monolayers on the basis of GISAXS inter-NPd. NDT ligands adopted a loop conformation according to kink defects observed in FT-IR.

Cyclic Voltammetry.

Drop-cast deposited solid-state electronic conductivity of surfactant-coated Au NP films was acquired in a CH Instruments 660 A (Austin, TX) electrochemical workstation. SNP film were casted on microlectrodes and CVs were run in a window potential from 300 to -300 mV and measured before and after liquid-phase exchanging the film with nonanedithiol ligands. The CV plot shows ~1 order of magnitude increase in current. Surprisingly, the film current changes from a predominant ionic/capacitive to ohmic current indicating that TOA^+ ligands were replaced and current throughout the film may occur by electron hopping despite the large separation between Au NPs observed in GISAXS.

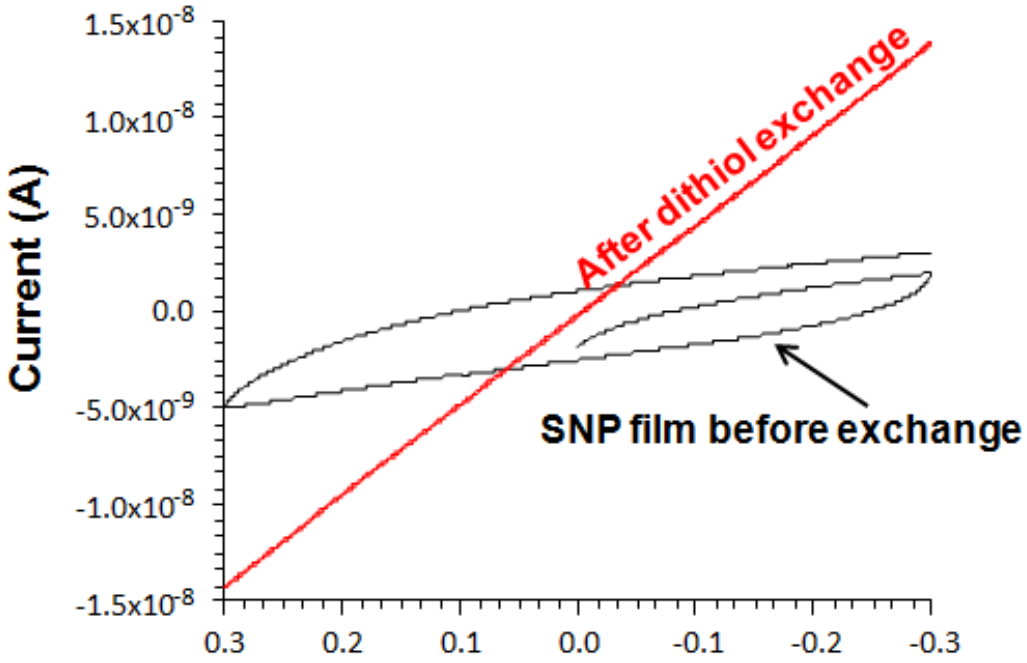

Figure S8. CV (*I vs. V*) before and after nonanedithiol exchange in the liquid-phase.

REFERENCES

(1) Sakka, S. Handbook of Sol-Gel Science and Technology: Processing, Characterization and Applications, V. I - Sol-Gel Processing/Hiromitsu Kozuka, Editor, V. II - Characterization of Sol-Gel Materials and Products/Rui M. Almeida, Editor, V. III - Applications of Sol-Gel Technology/Sumio Sakka, Editor; Springer, 2004.

(2) Rechberger, W.; Hohenau, A.; Leitner, A.; Krenn, J. R.; Lamprecht, B.; Aussenegg, F. R. Optical Properties of Two Interacting Gold Nanoparticles. Opt. Commun. **2003**, 220, 137–141.

(3) WangWang; Miller, D.; Fan, Q.; Luo, J.; Schadt, M.; Rendeng, Q.; Wang, G. R.; WangWang, J.; Kowach, G. R.; Zhong, C.-J. Assessment of Morphological and Optical Properties of Molecularly Mediated Thin Film Assembly of Gold Nanoparticles. J. Phys. Chem. C **2008**, 112, 2448–2455.